

RESEARCH

Open Access



Genome-wide detection of genetic structure and runs of homozygosity analysis in Anhui indigenous and Western commercial pig breeds using PorcineSNP80k data

Yao Jiang^{1†}, Xiaojin Li^{1†}, Jiali Liu², Wei Zhang¹, Mei Zhou¹, Jieru Wang¹, Linqing Liu¹, Shiguang Su¹, Fuping Zhao², Hongquan Chen³ and Chonglong Wang^{1*}

Abstract

Background: Runs of homozygosity (ROH) are continuous homozygous regions typically located in the DNA sequence of diploid organisms. Identifications of ROH that lead to reduced performance can provide valuable insight into the genetic architecture of complex traits. Here, we systematically investigated the population genetic structure of five Anhui indigenous pig breeds (AHIPs), and compared them to those of five Western commercial pig breeds (WECPs). Furthermore, we examined the occurrence and distribution of ROHs in the five AHIPs and estimated the inbreeding coefficients based on the ROHs (F_{ROH}) and homozygosity (F_{HOM}). Finally, we identified genomic regions with high frequencies of ROHs and annotated candidate genes contained therein.

Results: The WECPs and AHIPs were clearly differentiated into two separate clades consistent with their geographical origins, as revealed by the population structure and principal component analysis. We identified 13,530 ROHs across all individuals, of which 4,555 and 8,975 ROHs were unique to AHIPs and WECPs, respectively. Most ROHs identified in our study were short (< 10 Mb) or medium (10–20 Mb) in length. WECPs had significantly higher numbers of short ROHs, and AHIPs generally had longer ROHs. F_{ROH} values were significantly lower in AHIPs than in WECPs, indicating that breed improvement and conservation programmes were successful in AHIPs. On average, F_{ROH} and F_{HOM} values were highly correlated (0.952–0.991) in AHIPs and WECPs. A total of 27 regions had a high frequency of ROHs and contained 17 key candidate genes associated with economically important traits in pigs. Among these, nine candidate genes (*CCNT2*, *EGR2*, *MYL3*, *CDH13*, *PROX1*, *FLVCR1*, *SETD2*, *FGF18*, and *FGF20*) found in WECPs were related to muscular and skeletal development, whereas eight candidate genes (*CSN1S1*, *SULT1E1*, *TJP1*, *ZNF366*, *LIPC*, *MCEE*, *STAP1*, and *DUSP*) found in AHIPs were associated with health, reproduction, and fatness traits.

[†]Yao Jiang and Xiaojin Li contributed equally to this work.

*Correspondence: ahwchl@163.com

¹ Key Laboratory of Pig Molecular Quantitative Genetics of Anhui Academy of Agricultural Sciences, Anhui Provincial Key Laboratory of Livestock and Poultry Product Safety Engineering, Institute of Animal Husbandry and Veterinary Medicine, Anhui Academy of Agricultural Sciences, Hefei 230031, China

Full list of author information is available at the end of the article



Conclusion: Our findings provide a useful reference for the selection and assortative mating of pig breeds, laying the groundwork for future research on the population genetic structures of AHIPs, ultimately helping protect these local varieties.

Keywords: Anhui indigenous pig breeds, genetic structure, runs of homozygosity, Inbreeding coefficient, ROH island

Introduction

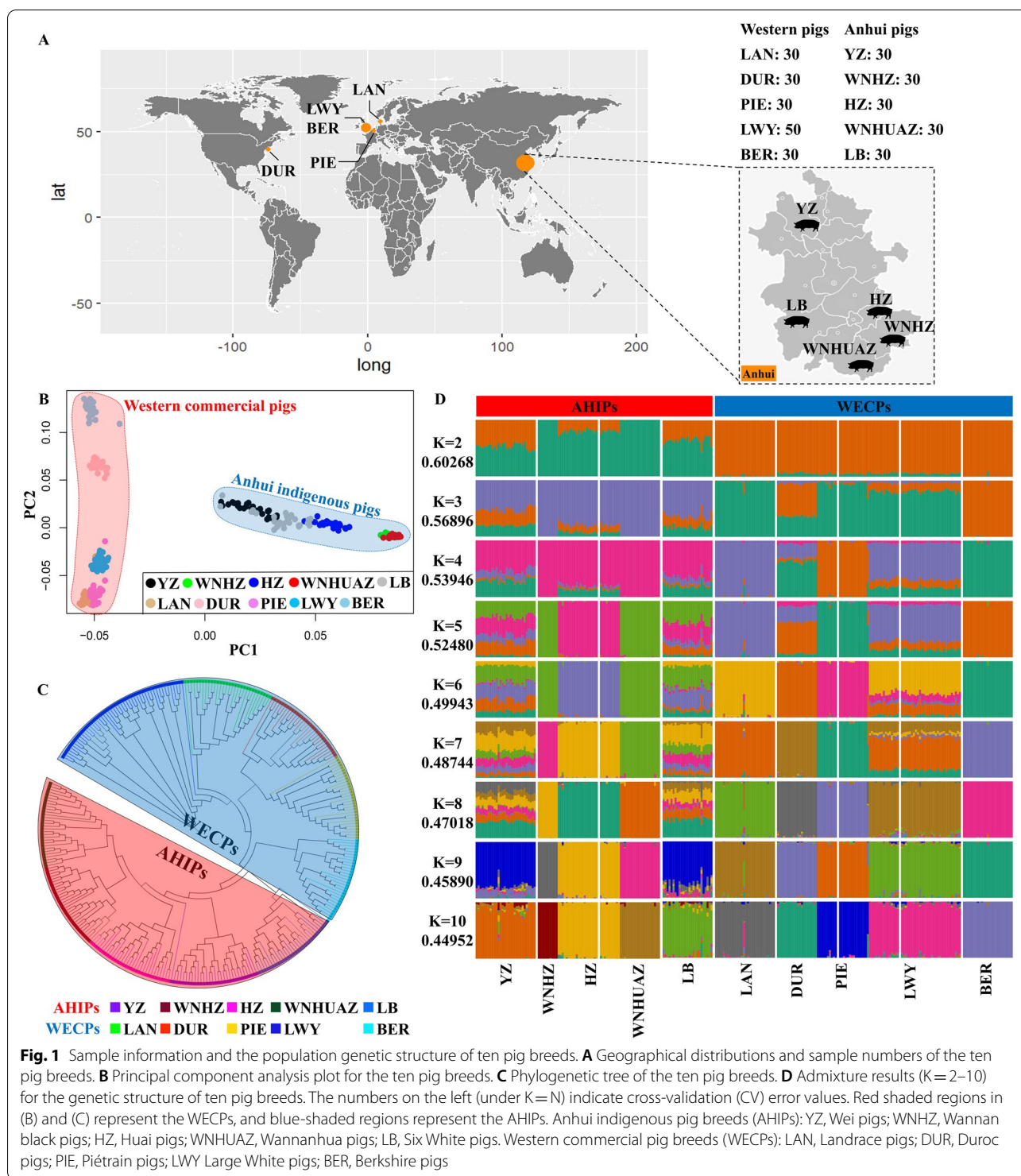
Runs of homozygosity (ROH) are defined as contiguous homozygous genotype segments present in an individual due to the parents transmitting identical haplotypes to their offspring [1]. Long ROHs are associated with more recent inbreeding within a pedigree, whereas short ROHs are associated with ancient common ancestors [2]. Bosse et al. [3] and Herrero et al. [4] used ROHs to investigate the population relationships, evolutionary history, and inbreeding effects in pigs. Several factors can influence the generation of ROHs, such as inbreeding, natural and artificial selection, genetic drift, and population bottlenecks. Of these, inbreeding is considered the most important factor [5]. Inbreeding leads to an increased risk of homozygosity for deleterious alleles throughout the genome, largely in the form of ROHs causing inbreeding depression, eventually leading to decreased fertility, viability, and phenotypic variation in the offspring [6]. Therefore, to avoid inbreeding depression in animal breeding programmes, a highly sensitive and accurate estimation of the inbreeding coefficient is of utmost importance [7].

Traditionally, the inbreeding coefficient has been estimated based on pedigree information (F_{PED}), whose accurate estimation relies heavily on the accuracy, completeness, and depth of pedigree information. However, pedigree errors are common in many livestock populations [8]. Several alternative methods have been proposed to estimate the genomic inbreeding coefficient (genomic F) based on the development of genotype-based microarrays using single nucleotide polymorphisms (SNPs). These include the genomic relationship matrix (F_{GRM}), homozygosity (F_{HOM}), and ROH (F_{ROH}). The genomic coefficients derived from animals/populations can be calculated without pedigree records or incomplete pedigree information. In addition, genomic F may provide a more accurate measure of inbreeding levels, even with missing pedigree information [9, 10]. Furthermore, compared with other genomic F indices, F_{ROH} is the most powerful and accurate method for detecting inbreeding effects and is closest to the true inbreeding coefficient [11, 12]. Thus, F_{ROH} has been widely used to estimate genomic inbreeding in livestock in recent years [13].

In pigs, ROH can also be used to estimate the inbreeding coefficient in the absence of pedigree

records. To date, ROH has been used to estimate inbreeding in several Western commercial pig breeds (WECPs), including Landrace (LAN) [14], Large White (LWY) [11], Piétrain (PIE) [15], and Duroc (DUC) breeds [16], as well as Chinese indigenous pig breeds, such as the Laiwu [17], Songliao black [18], Jinhua [19], Diannan small-ear [20], and Liangshan [21] breeds. Genomic regions with a high frequency of ROH (ROH islands) can also be used to detect associations between genes and economically important porcine traits. Previous reports have identified many genes associated with pig reproduction, meat quality, fat deposition, and disease resistance traits in ROH islands [17, 20, 22]. The presence of ROH islands in the porcine genome suggests the occurrence of selection for economically important traits and environmental adaptation.

Although ROH has been used for breeding estimates in many Western commercial and Chinese indigenous pig breeds, it has been used less frequently in Anhui indigenous pig breeds (AHIPs), including the Wei (YZ), Wannan black (WNHZ), Huai (HZ), Wannanhua (WNHUAZ), and Six White (LB). These breeds have improved meat quality [23], disease resistance [24], and high fertility [25] compared with major commercial lean pig breeds. Nevertheless, the number of AHIPs has declined sharply in the past 20 years due to the large number of Western pig breeds that have been imported to improve leanness in pork (China National Commission of Animal Genetic Resources, 2011). The African swine fever disease outbreak also caused problems for the breeding programmes. Thus, this study had the following aims: (1) to detect the differences in genetic structure between AHIPs and WECPs, including 150 AHIPs (YZ, WNHZ, HZ, WNHUAZ, and LB) and 170 WECPs (LAN, DUR, PIE, LWY, and BER (Berkshire)) using the Illumina porcine 80 K SNP BeadChip; (2) to identify the occurrence and distribution of ROHs in WECPs and AHIPs; (3) to calculate and compare the genomic inbreeding coefficients (F_{ROH}) between WECPs and AHIPs using ROHs; (4) to identify and compare potential ROH regions associated with economically important traits in AHIPs and WECPs. Our results could help preserve the genetic diversity of AHIPs, promoting sustainable breeding programmes for genetic improvement in these breeds.



Results

Analysis of population genetic structure of ten pig populations

Using the genetic background information of the ten pig breeds, we examined the relatedness among populations

of indigenous breeds (YZ, WNHZ, HZ, WNHUAZ, and LB) collected from Anhui Province, China. In addition, samples were collected from the five WECPs (LAN, LWY, BER, PIE, and DUR) and comparatively analysed (Fig. 1A). Principal component analysis (PCA) results

and phylogenetic trees were used to visualise the genetic relationships among the ten breeds (Fig. 1B, C). The PCA results showed that the AHIPs and WECs were clearly segregated along the PC1 axis. Furthermore, the five AHIP breeds were separated into four clusters, with WNHZ and WNHUAZ populations being classified together. Among the WECs, the BER, DUR, and LWY pigs clustered separately, whereas the LAN and PIE pigs clustered together. The phylogenetic tree had patterns similar to those of the PCA results, showing that overall, the AHIPs and WECs were distinguishable at the genomic level (Fig. 1C). The population genetic structure of the ten pig breeds ($K=2-10$ clusters) is illustrated in Fig. 1D. Based on the cross-validation ($CV=\text{minimal}$) error, we identified an optimal value of $K=10$ clusters, using which all ten pig breeds were clustered separately from each other. Using a $K=2$, all pig breeds were collectively separated into two distinct clusters—AHIPs and WECs. Taken together, the analysis results showed that the five AHIPs were closely related but had different genetic backgrounds, whereas the AHIPs and WECs significantly differed.

Distribution of runs of homozygosity

A descriptive summary of the ROH numbers and length categories (1–5 Mb, 5–10 Mb, 10–20 Mb, 20–40 Mb, and >40 Mb) in each pig breed is listed in Table 1 and illustrated in Fig. 2. All the LWY individuals exhibited at least one ROH longer than 1 Mb. Among the 13,530 ROHs identified, the majority were below 10 Mb in length, accounting for approximately 97.75% of the total ROHs (1–5 Mb: 56.05%; 5–10 Mb: 31.48%; 10–20 Mb: 10.21%; 20–30 Mb: 2.17%; >40 Mb: 0.08%) (Table 1, Fig. 1A). Moreover, the average ROH length was highest in HZ pigs (7.51 ± 0.28 Mb) and lowest in LWY pigs (4.86 ± 0.11 Mb). The average number of ROHs per pig was highest in BER pigs (70.20 ± 1.36 ; range, 54–88) and lowest in YZ pigs (15.00 ± 1.54 ; range, 4–40). The number of ROHs per chromosome tended to increase with chromosome length and was lowest on SSC11 and highest on SSC1 (Fig. 2B). Some BER, LAN, PIE, and WNHUAZ individuals had extremely long ROHs (>500 Mb) (Fig. 2C, D); in particular, one WHHUAZ individual had an ROH covering a total length of >600 Mb. Compared to the WECs, the AHIPs exhibited fewer total ROHs per individual (Fig. 1A). We also examined the total ROH numbers in each chromosome for all ten pig breeds (Fig. 2E). Compared to the AHIPs, the WECs contained more ROH fragments in all 18 chromosomes. Furthermore, the AHIPs had a lower proportion of short ROH fragments in the length categories of 1–5 Mb (29.79%), 5–10 Mb (34.94%), and 10–20 Mb (45.88%), while a higher proportion of length categories of 20–40 Mb (56.12%)

and >40 Mb (81.82%), suggesting recent inbreeding events (Table 1). Additionally, the percentage of chromosome coverage by ROH in each breed is summarised in Table S1 and illustrated in Figure S1. Among the WECs, the highest chromosome coverage by ROH was found in PIE (SSC18: 31.3%) and the lowest in SSC13 of LWY (SSC13: 5.4%). As for AHIPs, the highest was on chromosome 17 in WNHUAZ (29.6%), while the lowest was on chromosome 1 in LB (3.5%).

The descriptive statistics for ROH-based (F_{ROH}) and homozygous-based (F_{HOM}) inbreeding coefficients in different length categories are listed in Table 2 and illustrated in Fig. 3. The inbreeding coefficient of F_{HOM} varied from 0.0971 ± 0.0531 (LB) to 0.3079 ± 0.0492 (LAN), and the values of $F_{\text{ROH(ALL)}}$ varied from 0.064 ± 0.007 (YZ) to 0.289 ± 0.008 (LAN). We also found a high correlation between F_{HOM} and F_{ROH} in all ten breeds (range, 0.947–0.991), and the average correlation between F_{ROH} and F_{HOM} in the ten breeds was 0.967. The genomic inbreeding coefficients (F_{ROH} and F_{HOM}) were highest in the LAN, BER, and PIE breeds of WECs, and lowest in the HZ and YZ breeds of AHIPs (Fig. 3A, B). Similar conclusions drawn from F_{ROH} and F_{HOM} estimates indicated a considerable difference in genomic inbreeding coefficients among the different pig breeds. Of note, WECs had significantly higher genomic inbreeding coefficients than the AHIPs. These results showed that the F_{ROH} values differed significantly between the WEC and AHIP pig breeds, indicating differences in directional selection and breeding goals.

We identified the genomic regions most commonly associated with ROHs in the ten pig breeds and plotted the percentages of SNPs in ROHs against the positions of the SNPs along the chromosomes (Supplementary Fig. 2). No ROH islands were found in the LB and YZ breeds. High percentages of SNPs in ROHs were found in the BER (SSC1, SSC3, SSC6, SSC9, SSC12, SSC15), PIE (SSC4), and LAN (SSC7, SSC10, SSC14, SSC15) breeds. The longest ROH island (6.27 Mb) was found in the WNHUAZ breed on SSC1, whereas the shortest (0.05 Mb) was found in the HZ breed on SSC8. The SNPs in ROH islands were compared between WECs and AHIPs, and 220 and 748 unique SNPs were found in AHIPs and WECs, respectively (Fig. 4A). A total of 27 genomic regions had a high frequency of ROHs (Table S2) and were found to contain 202 genes. Among these, 48 candidate genes were found only in AHIPs, and 146 were found only in WECs (Fig. 4A). In addition, we aligned all of these ROH islands to the pig quantitative trait loci (QTL) database, revealing that meat-, carcass-, and production-related QTLs were enriched in 20 WEC genomic regions, while

Table 1 Summary of the number of runs of homozygosity (ROH) in different categories in each breed

Breed	N ^a	SNPs N ^b	Average Length (Mb)		Average Number		Categories (Mb)				
			Mean ± SE	Range	Mean ± SE	Range	1–5	5–10	10–20	20–40	>40
YZ	30	50–2607	6.27 ± 0.376	1.00 – 119.46	15.00 ± 1.54	4–40	218	145	58	19	3
WNHZ	30	50 – 2497	7.05 ± 0.242	1.04 – 120.98	38.20 ± 1.47	20–57	512	425	164	43	2
HZ	30	50 – 3084	7.51 ± 0.283	1.85 – 186.91	36.33 ± 1.63	19–53	506	370	181	32	1
WNHUAZ	30	50 – 2135	6.30 ± 0.206	1.00 – 113.53	44.00 ± 2.96	10–77	727	391	160	40	1
LB	30	50 – 3553	6.56 ± 0.420	1.02–192.42	18.57 ± 1.75	2–37	296	157	71	31	2
LAN	30	50 – 2309	6.41 ± 0.157	1.01–104.89	71.63 ± 2.82	10–94	1177	691	218	33	NA
DUR	30	50 – 1993	5.27 ± 0.135	1.01 – 75.95	40.03 ± 2.70	1–57	743	349	96	12	1
PIE	30	50 – 2107	5.62 ± >0.139	1.01–102.87	63.27 ± 4.50	1–91	1153	591	133	21	NA
LWY	50	50 – 3598	4.86 ± 0.110	1.00–134.02	33.02 ± 2.05	1–62	1085	439	113	14	NA
BER	30	50 – 3821	6.41 ± 0.194	1.44–225.01	70.20 ± 1.36	54–88	1167	701	188	49	1

Inbreeding coefficient of ROH (F_{ROH}) and homozygotes (F_{HOM})

^a Number of samples, N

^b Number of SNPs, SNPs N

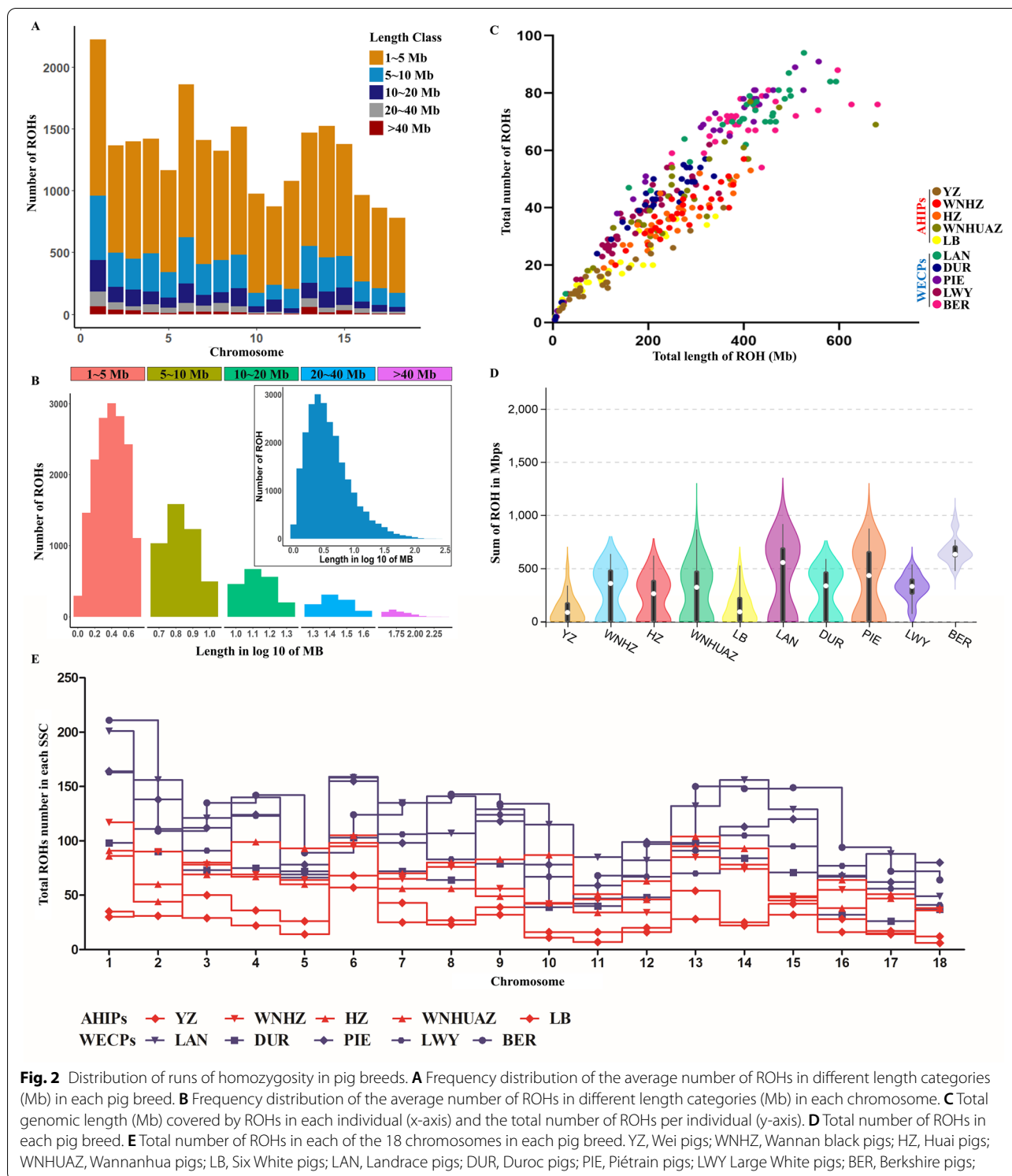
reproduction-, fatness-, and health-related QTLs were enriched in 7 AHIP genomic regions (Table S3).

GO enrichment analysis of candidate genes in WECPs and AHIPs

Gene Ontology (GO) enrichment analysis was performed separately for WECPs and AHIPs (Fig. 4B). Genes enriched in AHIPs were mainly involved in *blastocyst development*, *response to progesterone/oestrogen*, *positive regulation of B cell receptor signalling pathway*, and *triglyceride catabolic process*, whereas those in WECPs were involved in *skeletal muscle tissue development*, *embryonic skeletal system morphogenesis*, and *cellular response to growth factor stimulus*. Furthermore, nine candidate genes (*CCNT2*, *EGR2*, *MYL3*, *CDH13*, *PROX1*, *FLVCR1*, *SETD2*, *FGF18*, and *FGF20*) in WECPs were found to be closely associated ($P_{adj} < 0.05$) with *skeletal muscle tissue development*, *embryonic skeletal morphogenesis*, and *cellular response to growth factor stimulus*. Eight candidate genes (*CSN1S1*, *SULT1E1*, *TJP1*, *ZNF366*, *LIPC*, *MCEE*, *STAP1*, and *DUSP*) related to *sex hormones and reproductive development*, *fatty acid biosynthesis metabolism*, and *immune response regulation* were selected for subsequent analyses (Fig. 4C). Similarly, QTL enrichment results also revealed that ROH islands in two AHIP breeds (WHHUAZ and HZ) were associated with QTLs of economically important traits such as health, reproduction, and fatness, whereas those in the WECP breeds were related to meat- and production-related traits (Table 3).

Discussion

The Anhui Province is one of the top ten provinces that traditionally produce pigs in China, and it has abundant genetic resources of indigenous pig breeds (YZ, WNHZ, HZ, WNHUAZ, and LB). Due to long-term natural adaptation and artificial selection, the AHIPs have gradually evolved high fertility, high fat content, excellent meat quality [23], disease resistance [24], good maternal stability [25], and crude feed tolerance [22]. In this study, WECPs and AHIPs significantly differed in terms of genetic backgrounds, consistent with previous studies showing that pigs were domesticated in at least two separate domestication centres, Europe and Asia [26–28]. Noteworthy, artificial selection has also played a vital role in AHIPs, especially for LB/YZ breeds, as genomic information from Western breeds flowed into LB/YZ breeds. This could be because, in the past 20 years, WECPs were selected and admixed with AHIPs to increase the allelic richness and improve the breeding stock of AHIPs (China National Commission of Animal Genetic Resources, 2011). Besides, the WNHUAZ and WNHZ breeds exhibited a close genetic relationship, suggesting that both breeds may have descended from the same ancestor [29], and gradually formed two different breeds due to geographical isolation and the long-term domestication process [30]. Furthermore, the similar number of ROHs and F_{ROH} values in WNHUAZ and WNHZ also supported the notion that these breeds originated from a common population. However, due to the small sample size and marker density, the results of population genetic structure in the WECP and AHIP breeds are insufficient and need further investigation.



The abundance, length, and genomic distribution of ROHs provide valuable information about the demographic history of livestock species [3]. In this study, the occurrence and distribution of ROHs were compared

between five AHIPs and five WECPs. Most of the ROHs identified in our study belonged to the short (<10 Mb) and medium (10–20 Mb) length categories, consistent with those reported in chickens [31], sheep [32], pigs

Table 2 Descriptive statistics for runs of homozygosity (ROH) and inbreeding coefficients (F) in each breed

Breed	F _{ROH} (Mb, Mean ± SE)						F _{HOM}	r (F _{ROH} , F _{HOM})
	1–5	5–10	10–20	20–40	> 40	All		
YZ	0.046 ± 0.007	0.035 ± 0.006	0.030 ± 0.006	0.022 ± 0.004	0.021 ± 0.001	0.064 ± 0.007	0.0800 ± 0.0503	0.991
WNHZ	0.120 ± 0.006	0.094 ± 0.005	0.050 ± 0.004	0.022 ± 0.002	0.020	0.180 ± 0.003	0.2046 ± 0.0399	0.952
HZ	0.111 ± 0.006	0.086 ± 0.006	0.047 ± 0.005	0.021 ± 0.003	0.024	0.151 ± 0.002	0.1783 ± 0.0468	0.971
WNHUAZ	0.120 ± 0.011	0.086 ± 0.010	0.046 ± 0.007	0.024 ± 0.006	0.021	0.190 ± 0.010	0.2163 ± 0.0733	0.969
LB	0.057 ± 0.007	0.048 ± 0.007	0.033 ± 0.005	0.025 ± 0.003	0.021 ± 0.002	0.079 ± 0.007	0.0971 ± 0.0531	0.990
LAN	0.181 ± 0.010	0.130 ± 0.008	0.059 ± 0.005	0.017 ± 0.002	NA	0.289 ± 0.008	0.3079 ± 0.0610	0.967
DUR	0.092 ± 0.007	0.064 ± 0.005	0.027 ± 0.003	0.016 ± 0.002	0.018	0.165 ± 0.005	0.1809 ± 0.0549	0.947
PIE	0.152 ± 0.012	0.103 ± 0.009	0.043 ± 0.004	0.016 ± 0.001	NA	0.241 ± 0.009	0.2654 ± 0.0889	0.953
LWY	0.073 ± 0.005	0.046 ± 0.004	0.021 ± 0.003	0.015 ± 0.005	NA	0.123 ± 0.004	0.1443 ± 0.0532	0.968
BER	0.183 ± 0.008	0.128 ± 0.009	0.055 ± 0.008	0.026 ± 0.004	0.022	0.266 ± 0.001	0.3028 ± 0.0492	0.969

r(F_{ROH}, F_{HOM}), correlation between F_{ROH} and F_{HOM}; NA, no ROH was detected

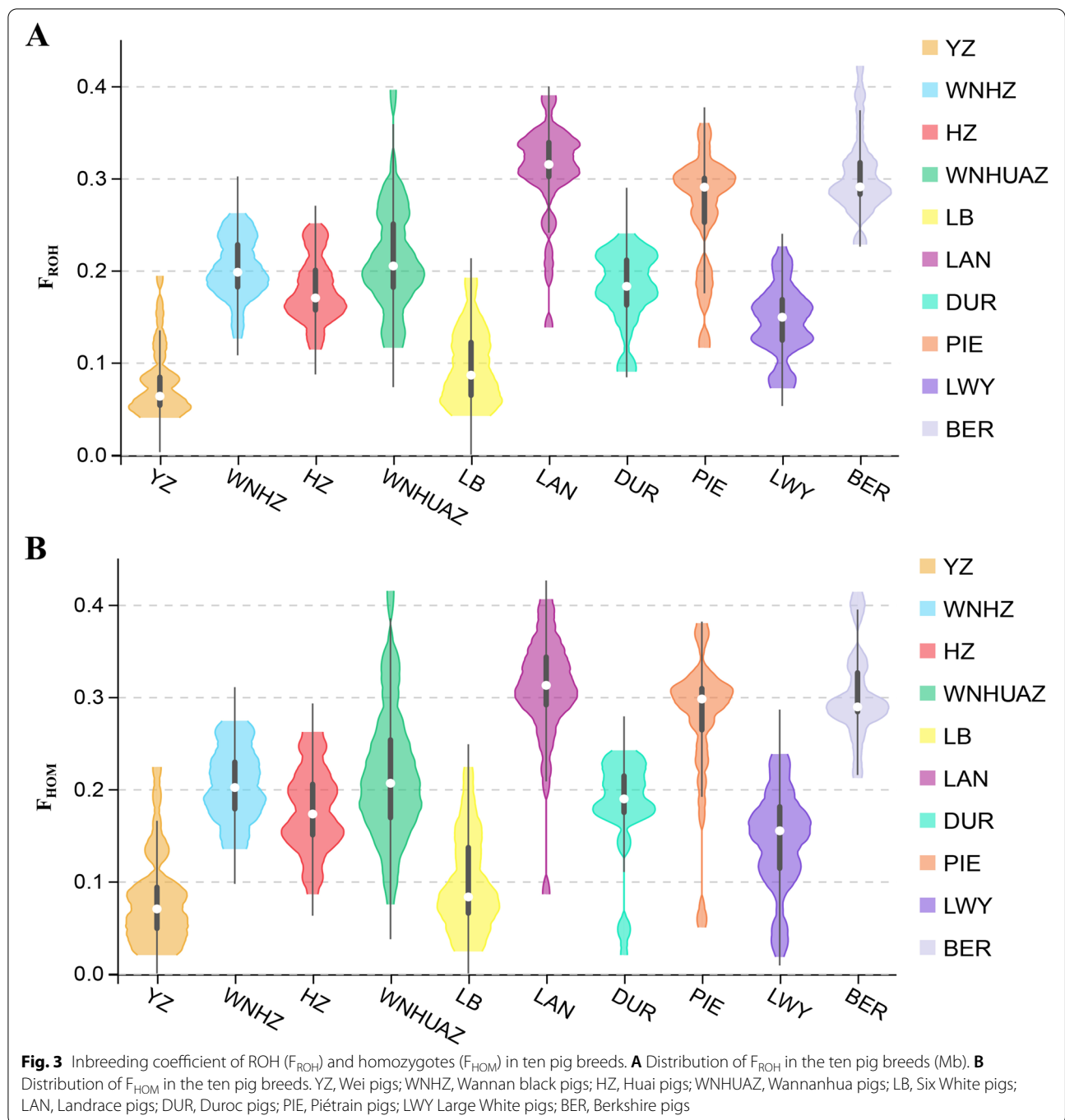
Genomic regions with a high frequency of ROHs

[18], and cattle [33]. The short ROHs indicate ancient inbreeding, whereas long ROHs suggest recent inbreeding [34]. Compared with WECPs, AHIPs had more ROHs in 20–40 Mb and > 40 Mb categories, fewer ROHs in 1–5 Mb and 5–10 Mb. These results are consistent with those of previous studies [18, 35]. The different distribution patterns of ROH numbers and lengths between the WECPs and AHIPs may be due to the selection of different traits in these breeds; WECP management primarily focuses on the production traits of pigs [36], whereas AHIPs are selected for meat quality and disease resistance [35].

With the development of high-throughput genotyping technologies, genetic markers can provide a more accurate estimate of population relationships in pigs than pedigree data, which may have missing or incorrect parent information [13, 22]. In recent years, ROHs have been widely used to predict inbreeding levels in livestock [13]. F_{ROH} estimates are more accurate for estimating autozygosity and detecting inbreeding effects than pedigree data [11], providing useful information about interindividual genetic relatedness. In this study, we used two indices, F_{ROH} and F_{HOM}, to estimate inbreeding coefficients in AHIPs and WECPs. Previous studies have reported that F_{ROH} generally highly correlates with F_{HOM} (r_{F_{ROH},F_{HOM}} = 0.78–0.85) consistent with our results (r_{F_{ROH},F_{HOM}} = 0.952–0.991) and previous studies [18, 37]. Moreover, we found that F_{HOM} values were higher than F_{ROH} values in all ten pig breeds because the F_{HOM} estimate cannot distinguish identity by descent alleles from identity by state alleles, inevitably overestimating inbreeding levels [38]. Although using F_{HOM} to estimate the inbreeding coefficient is not sufficiently accurate, F_{ROH} can alleviate the issues mentioned above. Thus, theoretically, F_{ROH} may be a more effective and accurate

alternative for quantifying relatedness and inbreeding levels [39]. Further, the F_{ROH} of AHIPs is generally expected to be lower than that of WECPs. The contradictory results of our study may be explained by the small effective population size and random sampling errors in WECPs, resulting in higher inbreeding estimates for WECPs in recent generations [40].

We found that the ROH islands harboured several candidate genes controlling economically important traits in pigs. In particular, we identified 27 genomic regions with a high frequency of ROHs, harbouring 17 key candidate genes in WECPs and AHIPs. Furthermore, we identified eight candidate genes in the AHIPs, of which three (*SULT1E1*, *LIPC*, and *MCEE*) were involved in fat deposition, three (*CSN1S1*, *TJP1*, and *ZNF366*) were involved in reproduction, and two (*STAP1* and *DUSP1*) were immune system-related. *LIPC* encodes hepatic lipase and affects the metabolism, composition, and expression of several lipoproteins [41, 42]. *SULT1E1*, a negative regulator of adipogenesis [43], serves a strong regulatory function in lipid metabolism via the PPARγ pathway [44]. *SULT1E1* is also reportedly linked to foetal development [45], and ablation of the murine *SULT1E1* gene causes placental thrombosis and spontaneous foetal loss [46]. *ZNF366* plays an important role in regulating the expression of target genes in response to oestrogen [47, 48]. *TJP1* has been related to testis weight, spermatogenesis, and the development of ovarian and cystic follicles [49, 50]. *CSN1S1* is an effective molecular marker for litter size in goat breeding [51]. *STAP1* [52] and *DUSP1* [53, 54] are significantly associated with anti-inflammatory responses and immune infiltration in human autoimmune diseases. We also identified nine candidate genes in the WECPs, of which six (*CDH13*, *PROX1*, *EGR2*, *CCNT2*, *SETD2*, and *MYL3*) were related to muscular



development, and three (*FLVCR1*, *FGF18*, and *FGF20*) were involved in skeletal morphogenesis. Among these candidate genes, miR-15a [55] and miR-155-5p [56] inhibit skeletal muscle development and differentiation by targeting *CCNT2*. High expression levels of *CDH13* promote muscle-type identity, as *CDH13* plays an active role in myogenesis [57, 58]. In pigs, *MYL3* [59, 60] and *EGR2* [61, 62] are associated with muscle formation and

development. *PROX1* is involved in muscle fibre conversion, and is a promising candidate gene affecting pork quality traits [59, 63]. *FGF18* [64, 65] and *FGF20* [66, 67] are reported to play important roles in embryonic development, bone growth, and bone-related diseases. Moreover, *FLVCR1* deficiency results in Diamond–Blackfan anaemia, often associated with skeletal malformations [68]. Based on the Pig QTL database, reproduction,

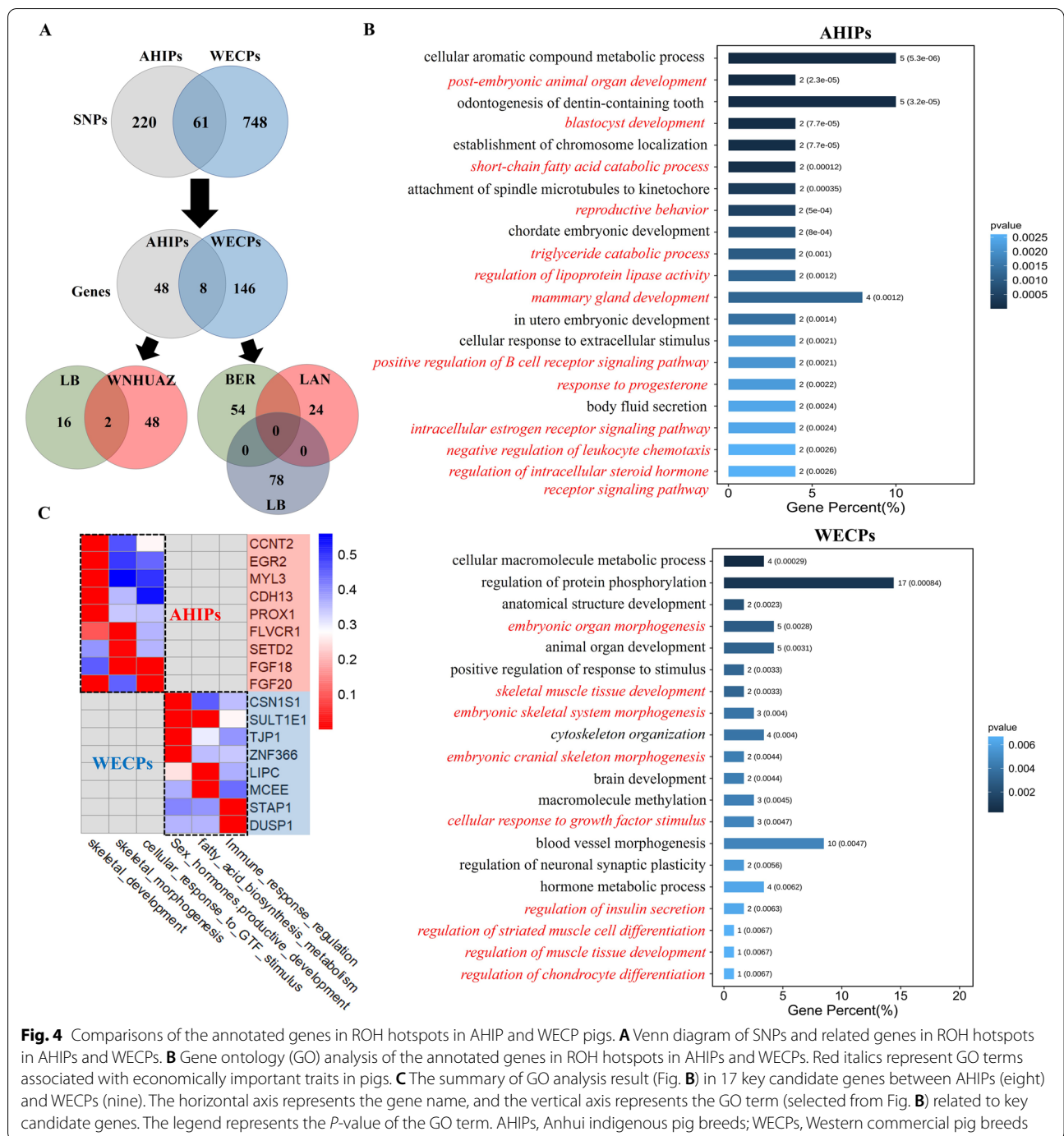


Fig. 4 Comparisons of the annotated genes in ROH hotspots in AHIP and WECP pigs. **A** Venn diagram of SNPs and related genes in ROH hotspots in AHIPs and WECPs. **B** Gene ontology (GO) analysis of the annotated genes in ROH hotspots in AHIPs and WECPs. Red italics represent GO terms associated with economically important traits in pigs. **C** The summary of GO analysis result (Fig. B) in 17 key candidate genes between AHIPs (eight) and WECPs (nine). The horizontal axis represents the gene name, and the vertical axis represents the GO term (selected from Fig. B) related to key candidate genes. The legend represents the *P*-value of the GO term. AHIPs, Anhui indigenous pig breeds; WECPs, Western commercial pig breeds

fatness, and health traits overlapped in the ROH islands of AHIPs, while meat- and production-related traits were observed within ROH islands of WECPs. Overall, we found that the AHIP breeds were more adapted to fat deposition, disease resistance, and high fertility, whereas WECP pigs showed selection for production traits, such as muscular and skeletal development. Taken together, our results indicate that the WECP and AHIP breeds

show adaptive differences in economically important traits.

Conclusions

In this study, we characterised the population genetic structure of WECPs and AHIPs and found that they had considerably different genetic backgrounds. Furthermore, the occurrence and distribution of ROHs were compared

Table 3 Candidate genes located in genomic regions with a high frequency of ROH associated with pig economic traits

Breed	CHR	Start (Mb)	End (Mb)	No SNPs	No genes	Candidate genes	Gene function	Traits related to QTL
BER	6	5.52	6.51	52	5	CDH13	Meat	Lean meat percentage (7632)
	9	129.04	130.63	81	9	PROX1	Meat	Carcass weight (12,786)
						FLVCR1	Meat/Production	Average daily gain (2896)
	14	65.87	68.09	48	7	EGR2	Meat	NA
	15	15.76	17.03	40	11	CCNT2	Meat	Meat colour score (3009)
17	4.39	5.63	54	10	FGF20	Meat/Production	Average daily gain (28,911)	
PIE	13	29.59	29.89	10	9	MYL3	Meat	Loin muscle area (5499)
						SETD2	Production	Body weight (21,843)
WNHUAZ	16	49.85	52.75	60	17	FGF18	Production	Average daily gain (28,900)
	1	111.18	117.45	86	6	LIPC	Fatness	Palmitoleic acid content (168,357)
						MCEE	Fatness	Intramuscular fat content (17,747)
	8	64.83	68.48	52	6	TJP1	Reproduction	Gestation length (10,617)
						STAP1	Health	Palmitoleic acid content (168,374)
ZNF366						Reproduction	Teat number (8812)	
16	48.62	51.50	47	15	DUSP1	Health	NA	
HZ	8	66.23	67.50	25	16	SULT1E1	Reproduction/Fatness	Teat number (124,206)
						CSN1S1	Reproduction	Corpus luteum number (492)

The distance between genes and ROH regions was calculated as follows: The starting coordinate of the gene minus the starting coordinate of the ROH region; all candidate genes are located in the ROH region; the number within brackets in the last column represents the QTL-ID

across five AHIPs and five WECPs. Results revealed how diversity has evolved in the AHIP populations. F_{ROH} and F_{HOM} values were significantly lower in AHIPs than in WECPs, indicating that the breeding and conservation programmes were successful in AHIPs. Several genes with a high frequency of ROHs were identified. Among these, candidate genes in AHIPs were associated with fat deposition, disease resistance, and high fertility, whereas those in WECPs were related to muscular and skeletal development. Overall, our findings provide a helpful reference for selection and assortative mating programmes in pigs. Moreover, these results reveal a novel research direction regarding the population genetic structure of AHIP breeds, which might effectively help protect these valuable local varieties.

Methods

SNP genotyping and quality control

A total of 320 pigs were used in this study: 170 WECPs (Duroc, Landrace, Yorkshire, Berkshire, and Piétrain pig breeds) and 150 AHIPs from the Anhui Province, China. Detailed information on the sampled pig breeds in this study, including the regions of recollection, breed names and abbreviations, and sample size, are presented in Table S4. Genomic DNA was extracted from

ear tissue and genotyped with the Illumina porcine 80 K SNP BeadChip (Illumina, San Diego, CA, USA). Only autosomal SNPs were used for further analyses. The PLINK software (v1.90) [69] was used for quality control of the data, and the following standards were set: (1) SNPs with a call rate of <0.95 and unknown positions were removed (*-geno 0.05*); (2) SNPs with a minor allele frequency of <0.05 were removed (*-maf 0.05*); (3) data from individuals with a call rate of <0.90 were discarded (*-mind 0.1*); (4) Hardy–Weinberg Equilibrium (HWE) P -value < 1×10^{-6} (*-hwe 0.000001*). The SNP genome coordinates were obtained from the Sus scrofa 11.1 porcine genome reference assembly. After genotype quality control, 1158 markers were excluded based on the HWE test ($p \leq 1 \times 10^{-6}$), 7231 SNPs failed the missingness test ($GENO > 0.1$), 9788 SNPs failed the frequency test ($MAF < 0.05$), yielding 320 individuals and 54,075 SNP for further analysis.

Population structure

The geographical distributions of five WECPs and five AHIPs were estimated using the *ggmap* package [70] in R statistical software. To illustrate the relationships among the ten pig breeds, PCA was performed using the GCTA software (*-autosome -autosome-num 18 -make-grm*

-pca 3) [71]. A scatterplot was generated to visualise the first and second principal components based on a variance-standardised relationship matrix created using the PCA results. The ADMIXTURE software [72] was used to infer the most probable number of ancestral populations ($K=2-10$) based on the SNP genotype data. A five-fold cross-validation (-cv) error for each K was used to select the optimal K . A phylogenetic tree was created for the ten pig breeds using the online tool, the Interactive Tree Of Life (iTOL, http://itol2.embl.de/personal_page.cgi) [73].

Genomic inbreeding coefficients

ROHs were identified for each individual using the PLINK software (v1.90), which uses a sliding window technique to scan each individual's genotype at each marker position to detect homozygous segments [39]. We defined ROHs according to the following criteria: (1) the minimum ROH length was set to 1 Mb (-homozyg-kb 1000); (2) a minimum of 50 consecutive SNPs were included in an ROH (-homozyg-snp 50), which was calculated using the equation proposed by Lencz et al. [74]:

$$l = \frac{\log_e \frac{\alpha}{n_s \times n_i}}{\log_e(1 - het)}$$

where α is the percentage of false-positive ROHs (set to 0.05 in the present study), n_s is the number of SNPs per individual, n_i is the number of individuals, and het is the heterozygosity across all SNPs. After calculation, the minimum number of SNPs constituting an ROH was set to 50; (3) the maximum gap between consecutive SNPs was set to 1 Mb (-homozyg-gap 1000); (4) the minimum SNP density was set to 1 SNP every 100 kb (-homozyg-density 100); (5) the minimum number of SNPs in a sliding window was set to 50 (-homozyg-snp 50); (6) one heterozygous genotype and no more than five missing SNPs were allowed per window (-homozyg-window-het 1; -homozyg-window-missing 5); (7) the window threshold was set to 0.01 (-homozyg-window-threshold 0.01). In this study, we classified ROHs into five different categories according to their physical length: 1 to <5 Mb, 5 to <10 Mb, 10 to <20 Mb, 20 to <40 Mb and >40 Mb. For each length category, we computed the frequency of ROH numbers and the average length of an ROH in every breed.

Inbreeding coefficient of ROH

To verify the accuracy of F_{ROH} , we evaluated the genomic coefficients for the ten pig breeds using two methods: (1) PLINK v1.90 software was used to measure the inbreeding coefficient based on the difference between the

observed and expected numbers of homozygous genotypes (F_{HOM}) [74]. The inbreeding coefficient for an individual (F_{HOM}) was calculated as follows:

$$F_{HOM} = \frac{(O - E)}{(L - E)}$$

where L is the number of genotyped autosomal SNPs, E is the number of homozygotes expected by chance, and O is the number of observed homozygotes. (2) Genomic inbreeding coefficients were also estimated based on ROH (F_{ROH}). The F_{ROH} was calculated as follows:

$$F_{HOM} = \frac{\sum_i L_{ROH_i}}{L_{auto}}$$

where L_{ROH_i} is the total length of ROH_i on autosomes, and L_{auto} is the autosomal genome length covered by the SNP chip. Furthermore, the correlation between F_{ROH} and F_{HOM} for each breed was calculated using Pearson's correlation.

Detection of common ROHs and gene annotation

To identify genomic regions with a high frequency of ROHs, we calculated the percentage of occurrences of SNPs in ROHs by counting the number of times an SNP was detected in those ROHs across individuals. In this study, the threshold used to define an ROH hotspot in the genome was 40%, in agreement with a previous report by Rui et al. [18]. Adjacent SNPs over this threshold were merged into genomic regions called ROH islands [75, 76]. We used the porcine reference genome annotation file from the NCBI database (http://asia.ensembl.org/Sus_scrofa/Info/Index) to annotate the genes in the ROH islands. In addition, pig QTLdb (<https://www.animalgenome.org/cgi-bin/QTLdb/SS/index>) was used to annotate the genes in the ROH islands. GO enrichment analysis of genes in the ROH islands was performed using g:Profiler (<https://biit.cs.ut.ee/gprofiler/gost>), and terms with a P -value greater than 0.05 were filtered. The biological function of each annotated gene within the ROH islands was determined through an extensive literature search.

Abbreviations

AHIPs: Anhui Indigenous Pig Breeds; WECBs: Western Commercial Pig Breeds; ROH: Runs of Homozygosity; F: Inbreeding Coefficient; SNP: Single Nucleotide Polymorphism; YZ: Wei; WNHz: Wannan Black; HZ: Huai; WNHAZ: Wannan-hua; LB: Six White; LAN: Landrace; DUR: Duroc; PIE: Piétrain; LWY: Large White; BER: Berkshire; PCA: Principal Component Analysis; CV: Cross-validation; SSC: Sus Scrofa Chromosome; CCNT2: Cyclin T2; EGR2: Early Growth Response 2; MYL3: Myosin Light Chain 3; CDH13: Cadherin 13; PROX1: Prospero Homeobox; 1; FLVCR1: FLVCR heme transporter 1; SETD2: SET domain containing 2, histone lysine methyltransferase; FGF18: Fibroblast Growth Factor 18; FGF20: Fibroblast Growth Factor 20; CSN1S1: Casein Alpha S1; SULT1E1: Sulfotransferase Family 1E, Oestrogen-preferring, Member 1; TJP1: Tight Junction Protein 1; ZNF366: Zinc Finger Protein 366; LIPC: Lipase C Hepatic Type; MCEE:

Methylmalonyl-CoA Epimerase; STAP1: Signal Transducing Adaptor Family Member 1; DUSP1: Dual Specificity Phosphatase 1.

Supplementary Information

The online version contains supplementary material available at <https://doi.org/10.1186/s12864-022-08583-9>.

Additional file 1: SupplementaryFigure 1. The percentage of chromosome coverage (%) by ROHs in each breed. YZ, Wei pigs; WNHZ, Wannan black pigs; HZ, Huai pigs; WNHUAZ, Wannanhua pigs; LB, Six White pigs; LAN, Landrace pigs; DUR, Duroc pigs; PIE, Piétrain pigs; LWY Large White pigs; BER, Berkshire pigs.

Additional file 2: SupplementaryFigure 2. Manhattan plot of the occurrence (%) of SNPs in ROHs in ten pig breeds. The x-axis represents the SNP genomic coordinate in each chromosome, and the y-axis shows the proportion of overlapping ROHs shared among individuals, based upon the number in population. Colourful data points indicate SNPs, and the dashed line represents the 40% threshold. YZ, Wei pigs; WNHZ, Wannan black pigs; HZ, Huai pigs; WNHUAZ, Wannanhua pigs; LB, Six White pigs; LAN, Landrace pigs; DUR, Duroc pigs; PIE, Piétrain pigs; LWY Large White pigs; BER, Berkshire pigs.

Additional file 3: Supplemental Table 1. The percentage of chromosome coverage (%) by ROHs in each breed. **Supplemental Table 2.** Candidate genes located in genomic regions with a high frequency of ROHs. **Supplemental Table 3.** Pig QTLs located in genomic regions with a high frequency of ROHs. **Supplemental Table 4.** The summary of Sample information for each breed.

Acknowledgements

The authors gratefully acknowledge the constructive comments from reviewers.

Authors' contributions

HQC and CLW conceived the study. MZ and WZ collected the samples and recorded the phenotypes. XJL and JY performed analysis. JLL and JRW contributed to the visualisation of the data. FPZ, LQL, and SGS supervised the study and proposed revisions to the manuscript. YJ and CLW wrote and revised the manuscript. All authors read and approved the manuscript.

Funding

This work was supported by grants from the Anhui Academy of Agricultural Sciences Key Laboratory Project (No.2021YL023), The 68th China Postdoctoral Science Foundation Project (No.2020M681977), 2020 Anhui Postdoctoral Research Project (No. 2020A394), Anhui Natural Science Foundation (No.2008085QC138), Anhui Swine Industry Technology System Project (AHCYTX-05-15), Anhui Province Financial Modern Seed Industry Development Fund Project and Anhui Natural Science Foundation (No. 2108085QC135).

Availability of data and materials

The datasets used and/or analysed during the current study are available from the corresponding author on reasonable request.

Declarations

Ethics approval and consent to participate

The experiments were performed according to the Regulations for the Administration of Affairs Concerning Experimental Animals and approved by the Animal Research Committee of the Anhui Academy of Agriculture Sciences.

Consent for publication

Not applicable.

Competing interests

The authors declare that they have no competing interests.

Author details

¹Key Laboratory of Pig Molecular Quantitative Genetics of Anhui Academy of Agricultural Sciences, Anhui Provincial Key Laboratory of Livestock and Poultry Product Safety Engineering, Institute of Animal Husbandry and Veterinary Medicine, Anhui Academy of Agricultural Sciences, Hefei 230031, China. ²Key Laboratory of Animal Genetics, Breeding and Reproduction (Poultry) of Ministry of Agriculture, Institute of Animal Science, Chinese Academy of Agricultural Sciences, Beijing 100193, China. ³College of Animal Science and Technology, Anhui Agricultural University, Hefei 230036, China.

Received: 18 November 2021 Accepted: 22 April 2022

Published online: 17 May 2022

References

- Gibson J, Morton NE, Collins A. Extended tracts of homozygosity in outbred human populations. *Hum Mol Genet.* 2006;15(5):789–95.
- Szpiech ZA, Xu J, Pemberton TJ, Peng W, Zollner S, Rosenberg NA, Li JZ. Long runs of homozygosity are enriched for deleterious variation. *Am J Hum Genet.* 2013;93(1):90–102.
- Bosse M, Megens HJ, Madsen O, Paudel Y, Frantz LA, Schook LB, Crooijmans RP, Groenen MA. Regions of homozygosity in the porcine genome: consequence of demography and the recombination landscape. *PLoS Genet.* 2012;8(11):e1003100.
- Herrero-Medrano JM, Megens HJ, Groenen MA, Ramis G, Bosse M, Perez-Enciso M, Crooijmans RP. Conservation genomic analysis of domestic and wild pig populations from the Iberian Peninsula. *BMC Genet.* 2013;14:106.
- Keller MC, Visscher PM, Goddard ME. Quantification of inbreeding due to distant ancestors and its detection using dense single nucleotide polymorphism data. *Genetics.* 2011;189(1):237–49.
- Ku CS, Naidoo N, Teo SM, Pawitan Y. Regions of homozygosity and their impact on complex diseases and traits. *Hum Genet.* 2011;129(1):1–15.
- Ferencakovic M, Hamzic E, Gredler B, Solberg TR, Klemetsdal G, Curik I, Solkner J. Estimates of autozygosity derived from runs of homozygosity: empirical evidence from selected cattle populations. *J Anim Breed Genet.* 2013;130(4):286–93.
- Wang L, Sorensen P, Janss L, Ostensen T, Edwards D. Genome-wide and local pattern of linkage disequilibrium and persistence of phase for 3 Danish pig breeds. *BMC Genet.* 2013;14:115.
- Purfield DC, Berry DP, McParland S, Bradley DG. Runs of homozygosity and population history in cattle. *BMC Genet.* 2012;13:70.
- Ferencakovic M, Solkner J, Kaps M, Curik I. Genome-wide mapping and estimation of inbreeding depression of semen quality traits in a cattle population. *J Dairy Sci.* 2017;100(6):4721–30.
- Shi L, Wang L, Liu J, Deng T, Yan H, Zhang L, Liu X, Gao H, Hou X, Wang L, et al. Estimation of inbreeding and identification of regions under heavy selection based on runs of homozygosity in a Large White pig population. *J Anim Sci Biotechnol.* 2020;11:46.
- Forutan M, Ansari Mahyari S, Baes C, Melzer N, Schenkel FS, Sargolzaei M. Inbreeding and runs of homozygosity before and after genomic selection in North American Holstein cattle. *BMC Genomics.* 2018;19(1):98.
- Peripolli E, Munari DP, Silva M, Lima ALF, Irgang R, Baldi F. Runs of homozygosity: current knowledge and applications in livestock. *Anim Genet.* 2017;48(3):255–71.
- Joaquim LB, Chud TCS, Marchesi JAP, Savegnago RP, Buzanskas ME, Zanella R, Cantao ME, Peixoto JO, Ledur MC, Irgang R, et al. Genomic structure of a crossbred Landrace pig population. *PLoS ONE.* 2019;14(2):e0212266.
- Zhan H, Zhang S, Zhang K, Peng X, Xie S, Li X, Zhao S, Ma Y. Genome-Wide Patterns of Homozygosity and Relevant Characterizations on the Population Structure in Pietrain Pigs. *Genes (Basel).* 2020;11(5):577.
- Schiavo G, Bovo S, Bertolini F, Tinarelli S, Dall'Olio S, Nanni Costa L, Gallo M, Fontanesi L. Comparative evaluation of genomic inbreeding parameters in seven commercial and autochthonous pig breeds. *Animal.* 2020;14(5):910–20.
- Fang Y, Hao X, Xu Z, Sun H, Zhao Q, Cao R, Zhang Z, Ma P, Sun Y, Qi Z, et al. Genome-Wide Detection of Runs of Homozygosity in Laiwu Pigs Revealed by Sequencing Data. *Front Genet.* 2021;12:629966.

18. Xie R, Shi L, Liu J, Deng T, Wang L, Liu Y, Zhao F. Genome-Wide Scan for Runs of Homozygosity Identifies Candidate Genes in Three Pig Breeds. *Animals (Basel)*. 2019;9(8):518.
19. Xu Z, Sun H, Zhang Z, Zhao Q, Olasege BS, Li Q, Yue Y, Ma P, Zhang X, Wang Q, et al. Assessment of Autozygosity Derived From Runs of Homozygosity in Jinhua Pigs Disclosed by Sequencing Data. *Front Genet*. 2019;10:274.
20. Wu F, Sun H, Lu S, Gou X, Yan D, Xu Z, Zhang Z, Qadri QR, Zhang Z, Wang Z, et al. Genetic Diversity and Selection Signatures Within Diannan Small-Ear Pigs Revealed by Next-Generation Sequencing. *Front Genet*. 2020;11:733.
21. Liu B, Shen L, Guo Z, Gan M, Chen Y, Yang R, Niu L, Jiang D, Zhong Z, Li X, et al. Single nucleotide polymorphism-based analysis of the genetic structure of Liangshan pig population. *Anim Biosci*. 2021;34(7):1105–15.
22. Zhang W, Yang M, Zhou M, Wang Y, Wu X, Zhang X, Ding Y, Zhao G, Yin Z, Wang C. Identification of Signatures of Selection by Whole-Genome Resequencing of a Chinese Native Pig. *Front Genet*. 2020;11:566255.
23. Li Q, Huang Z, Zhao W, Li M, Li C. Transcriptome Analysis Reveals Long Intergenic Non-Coding RNAs Contributed to Intramuscular Fat Content Differences between Yorkshire and Wei Pigs. *Int J Mol Sci*. 2020;21(5):1732.
24. Ding X, Zhang X, Yang Y, Ding Y, Xue W, Meng Y, Zhu W, Yin Z. Polymorphism, Expression of Natural Resistance-associated Macrophage Protein 1 Encoding Gene (NRAMP1) and Its Association with Immune Traits in Pigs. *Asian-Australas J Anim Sci*. 2014;27(8):1189–95.
25. Zhang XD, Zhu HY, Zhou J, Wang N, Zhou N, Huang L, Wu T, Feng YF, Ding YY, Yin ZJ. Relationship between polymorphisms in exon 10 of FSHR gene and litter size in swine. *Genet Mol Res*. 2015;14(3):8252–61.
26. Giuffra E, Kijas JM, Amarger V, Carlborg O, Jeon JT, Andersson L. The origin of the domestic pig: independent domestication and subsequent introgression. *Genetics*. 2000;154(4):1785–91.
27. Larson G, Dobney K, Albarella U, Fang M, Matisoo-Smith E, Robins J, Lowden S, Finlayson H, Brand T, Willerslev E, et al. Worldwide phylogeography of wild boar reveals multiple centers of pig domestication. *Science*. 2005;307(5715):1618–21.
28. Li M, Chen L, Tian S, Lin Y, Tang Q, Zhou X, Li D, Yeung CKL, Che T, Jin L, et al. Comprehensive variation discovery and recovery of missing sequence in the pig genome using multiple de novo assemblies. *Genome Res*. 2017;27(5):865–74.
29. Wu X, Zhou R, Zhang W, Cao B, Xia J, Wang C, Zhang X, Chu M, Yin Z, Ding Y. Genome-wide scan for runs of homozygosity identifies candidate genes in Wannan Black pigs. *Anim Biosci*. 2021;34(12):1895–902.
30. Li XJ, Liu LQ, Dong H, Yang JJ, Wang WW, Zhang Q, Wang CL, Zhou J, Chen HQ. Comparative genome-wide methylation analysis of longissimus dorsi muscles in Yorkshire and Wannanhu pigs. *Anim Genet*. 2021;52(1):78–89.
31. Talebi R, Szmatala T, Meszaros G, Qanbari S. Runs of Homozygosity in Modern Chicken Revealed by Sequence Data. *G3 (Bethesda)*. 2020;10(12):4615–23.
32. Dzomba EF, Chimonyo M, Pierneef R, Muchadeyi FC. Runs of homozygosity analysis of South African sheep breeds from various production systems investigated using OvineSNP50k data. *BMC Genomics*. 2021;22(1):7.
33. Szmatala T, Gurgul A, Jasielczuk I, Zabek T, Ropka-Molik K, Litwinczuk Z, Bugno-Poniewierska M. A Comprehensive Analysis of Runs of Homozygosity of Eleven Cattle Breeds Representing Different Production Types. *Animals (Basel)*. 2019;9(12):1024.
34. Kirin M, McQuillan R, Franklin CS, Campbell H, McKeigue PM, Wilson JF. Genomic runs of homozygosity record population history and consanguinity. *PLoS ONE*. 2010;5(11):e13996.
35. Zhang Z, Zhang Q, Xiao Q, Sun H, Gao H, Yang Y, Chen J, Li Z, Xue M, Ma P, et al. Distribution of runs of homozygosity in Chinese and Western pig breeds evaluated by reduced-representation sequencing data. *Anim Genet*. 2018;49(6):579–91.
36. Bovo S, Ribani A, Munoz M, Alves E, Araujo JP, Bozzi R, Candek-Potokar M, Charneca R, Di Palma F, Etherington G, et al. Whole-genome sequencing of European autochthonous and commercial pig breeds allows the detection of signatures of selection for adaptation of genetic resources to different breeding and production systems. *Genet Sel Evol*. 2020;52(1):33.
37. Peripolli E, Stafuzza NB, Munari DP, Lima ALF, Irgang R, Machado MA, Panetto J, Ventura RV, Baldi F, da Silva M. Assessment of runs of homozygosity islands and estimates of genomic inbreeding in Gyr (*Bos indicus*) dairy cattle. *BMC Genomics*. 2018;19(1):34.
38. Wang J. Marker-based estimates of relatedness and inbreeding coefficients: an assessment of current methods. *J Evol Biol*. 2014;27(3):518–30.
39. Howrigan DP, Simonson MA, Keller MC. Detecting autozygosity through runs of homozygosity: a comparison of three autozygosity detection algorithms. *BMC Genomics*. 2011;12:460.
40. Curik I, Ferencakovic M, Solkner J. Inbreeding and runs of homozygosity: A possible solution to an old problem. *Livest Sci*. 2014;166:26–34.
41. Teng MS, Wu S, Hsu LA, Tzeng IS, Chou HH, Su CW, Ko YL. Pleiotropic association of LIPC variants with lipid and urinary 8-hydroxy deoxyguanosine levels in a Taiwanese population. *Lipids Health Dis*. 2019;18(1):111.
42. Guerra-García MT, Moreno-Macias H, Ochoa-Guzman A, Ordóñez-Sánchez ML, Rodríguez-Guillen R, Vázquez-Cardenas P, Ortiz-Ortega VM, Peimbert-Torres M, Aguilar-Salinas CA, Tusie-Luna MT. The -514C>T polymorphism in the LIPC gene modifies type 2 diabetes risk through modulation of HDL-cholesterol levels in Mexicans. *J Endocrinol Invest*. 2021;44(3):557–65.
43. Wada T, Ihunnah CA, Gao J, Chai X, Zeng S, Philips BJ, Rubin JP, Marra KG, Xie W. Estrogen sulfotransferase inhibits adipocyte differentiation. *Mol Endocrinol*. 2011;25(9):1612–23.
44. Xu Y, Yang X, Wang Z, Li M, Ning Y, Chen S, Yin L, Li X. Estrogen sulfotransferase (SULT1E1) regulates inflammatory response and lipid metabolism of human endothelial cells via PPARgamma. *Mol Cell Endocrinol*. 2013;369(1–2):140–9.
45. Duanmu Z, Weckle A, Koukouritaki SB, Hines RN, Falany JL, Falany CN, Kocarek TA, Runge-Morris M. Developmental expression of aryl, estrogen, and hydroxysteroid sulfotransferases in pre- and postnatal human liver. *J Pharmacol Exp Ther*. 2006;316(3):1310–7.
46. Tong MH, Jiang H, Liu P, Lawson JA, Brass LF, Song WC. Spontaneous fetal loss caused by placental thrombosis in estrogen sulfotransferase-deficient mice. *Nat Med*. 2005;11(2):153–9.
47. Borghese B, Tost J, de Surville M, Busato F, Letourneur F, Mondon F, Vaiman D, Chapron C. Identification of susceptibility genes for peritoneal, ovarian, and deep infiltrating endometriosis using a pooled sample-based genome-wide association study. *Biomed Res Int*. 2015;2015: 461024.
48. Ruiz-Larranaga O, Langa J, Rendo F, Manzano C, Iriondo M, Estonba A. Genomic selection signatures in sheep from the Western Pyrenees. *Genet Sel Evol*. 2018;50(1):9.
49. Zhang L, Feng T, Spicer LJ. The role of tight junction proteins in ovarian follicular development and ovarian cancer. *Reproduction*. 2018;155(4):R183–98.
50. Aldahhan RA, Stanton PG, Ludlow H, de Kretser DM, Hedger MP. Acute heat-treatment disrupts inhibin-related protein production and gene expression in the adult rat testis. *Mol Cell Endocrinol*. 2019;498:110546.
51. Wang K, Yan H, Xu H, Yang Q, Zhang S, Pan C, Chen H, Zhu H, Liu J, Qu L, et al. A novel indel within goat casein alpha S1 gene is significantly associated with litter size. *Gene*. 2018;671:161–9.
52. Steeghs EMP, Bakker M, Hoogkamer AQ, Boer JM, Hartman QJ, Stalpers F, Escherich G, de Haas V, de Groot-Kruseman HA, Pieters R, et al. High STAP1 expression in DUX4-rearranged cases is not suitable as therapeutic target in pediatric B-cell precursor acute lymphoblastic leukemia. *Sci Rep*. 2018;8(1):693.
53. Zhang J, Chen Y, Namani A, Elshaer M, Jiang Z, Shi H, Tang X, Wang XJ. Comparative transcriptome analysis reveals Dusp1 as a critical regulator of inflammatory response to fly ash particle exposure in mouse. *Ecotoxicol Environ Saf*. 2020;190:110116.
54. Bai Q, Liu H, Guo H, Lin H, Song X, Jin Y, Liu Y, Guo H, Liang S, Song R, et al. Identification of Hub Genes Associated With Development and Microenvironment of Hepatocellular Carcinoma by Weighted Gene Co-expression Network Analysis and Differential Gene Expression Analysis. *Front Genet*. 2020;11:615308.
55. Teng Y, Wang Y, Fu J, Cheng X, Miao S, Wang L. Cyclin T2: a novel miR-15a target gene involved in early spermatogenesis. *FEBS Lett*. 2011;585(15):2493–500.
56. Xu S, Chang Y, Wu G, Zhang W, Man C. Potential role of miR-155-5p in fat deposition and skeletal muscle development of chicken. *Biosci Rep*. 2020;40(6): BSR20193796.
57. Poliak S, Norovich AL, Yamagata M, Sanes JR, Jessell TM. Muscle-type Identity of Proprioceptors Specified by Spatially Restricted Signals from Limb Mesenchyme. *Cell*. 2016;164(3):512–25.
58. Tamas M, Pankratova S, Schjerling P, Soendenbroe C, Yeung CC, Pennisi CP, Jakobsen JR, Krosgaard MR, Kjaer M, Mackey AL. Mutual stimulatory signaling between human myogenic cells and rat cerebellar neurons. *Physiol Rep*. 2021;9(21): e15077.

59. Chen G, Su Y, Cai Y, He L, Yang G. Comparative transcriptomic analysis reveals beneficial effect of dietary mulberry leaves on the muscle quality of finishing pigs. *Vet Med Sci*. 2019;5(4):526–35.
60. Wang Z, Shang P, Li Q, Wang L, Chamba Y, Zhang B, Zhang H, Wu C. iTRAQ-based proteomic analysis reveals key proteins affecting muscle growth and lipid deposition in pigs. *Sci Rep*. 2017;7:46717.
61. Munoz M, Garcia-Casco JM, Caraballo C, Fernandez-Barroso MA, Sanchez-Esquiliche F, Gomez F, Rodriguez MDC, Sillio L. Identification of Candidate Genes and Regulatory Factors Underlying Intramuscular Fat Content Through Longissimus Dorsi Transcriptome Analyses in Heavy Iberian Pigs. *Front Genet*. 2018;9:608.
62. Song SQ, Ma WW, Zeng SX, Zhang CL, Yan J, Sun CC, Li X, Wang RM, Li ZQ. Transcriptome analysis of differential gene expression in the longissimus dorsi muscle from Debao and landrace pigs based on RNA-sequencing. *Biosci Rep*. 2019;39(12):BSR20192144.
63. Petchey LK, Risebro CA, Vieira JM, Roberts T, Bryson JB, Greensmith L, Lythgoe MF, Riley PR. Loss of Prox1 in striated muscle causes slow to fast skeletal muscle fiber conversion and dilated cardiomyopathy. *Proc Natl Acad Sci U S A*. 2014;111(26):9515–20.
64. Hung IH, Schoenwolf GC, Lewandoski M, Ornitz DM. A combined series of Fgf9 and Fgf18 mutant alleles identifies unique and redundant roles in skeletal development. *Dev Biol*. 2016;411(1):72–84.
65. Wang J, Liu S, Li J, Yi Z. The role of the fibroblast growth factor family in bone-related diseases. *Chem Biol Drug Des*. 2019;94(4):1740–9.
66. Levy R, Mott RF, Iraqi FA, Gabet Y. Collaborative cross mice in a genetic association study reveal new candidate genes for bone microarchitecture. *BMC Genomics*. 2015;16:1013.
67. Huang J, Wang K, Shiflett LA, Brotto L, Bonewald LF, Wacker MJ, Dallas SL, Brotto M. Fibroblast growth factor 9 (FGF9) inhibits myogenic differentiation of C2C12 and human muscle cells. *Cell Cycle*. 2019;18(24):3562–80.
68. Mercurio S, Aspesi A, Silengo L, Altruda F, Dianzani I, Chiabrando D. Alteration of heme metabolism in a cellular model of Diamond-Blackfan anemia. *Eur J Haematol*. 2016;96(4):367–74.
69. Purcell S, Neale B, Todd-Brown K, Thomas L, Ferreira MA, Bender D, Maller J, Sklar P, de Bakker PI, Daly MJ, et al. PLINK: a tool set for whole-genome association and population-based linkage analyses. *Am J Hum Genet*. 2007;81(3):559–75.
70. Kahle D, Wickham H. Ggmap: Spatial visualization with ggplot2. *CONTRIBUTED RESEARCH ARTICLES*. 2013;5:144–61.
71. Yang J, Lee SH, Goddard ME, Visscher PM. GCTA: a tool for genome-wide complex trait analysis. *Am J Hum Genet*. 2011;88(1):76–82.
72. Alexander DH, Novembre J, Lange K. Fast model-based estimation of ancestry in unrelated individuals. *Genome Res*. 2009;19(9):1655–64.
73. Letunic I, Bork P. Interactive Tree Of Life (iTOL): an online tool for phylogenetic tree display and annotation. *Bioinformatics*. 2007;23(1):127–8.
74. Lencz T, Lambert C, DeRosse P, Burdick KE, Morgan TV, Kane JM, Kucherlapati R, Malhotra AK. Runs of homozygosity reveal highly penetrant recessive loci in schizophrenia. *Proc Natl Acad Sci U S A*. 2007;104(50):19942–7.
75. Purfield DC, McParland S, Wall E, Berry DP. The distribution of runs of homozygosity and selection signatures in six commercial meat sheep breeds. *PLoS ONE*. 2017;12(5):e0176780.
76. Mastrangelo S, Ciani E, Sardina MT, Sottile G, Pilla F, Portolano B, Bi.Ov. Ita C. Runs of homozygosity reveal genome-wide autozygosity in Italian sheep breeds. *Anim Genet*. 2018;49(1):71–81.

Publisher's Note

Springer Nature remains neutral with regard to jurisdictional claims in published maps and institutional affiliations.

Ready to submit your research? Choose BMC and benefit from:

- fast, convenient online submission
- thorough peer review by experienced researchers in your field
- rapid publication on acceptance
- support for research data, including large and complex data types
- gold Open Access which fosters wider collaboration and increased citations
- maximum visibility for your research: over 100M website views per year

At BMC, research is always in progress.

Learn more biomedcentral.com/submissions

